# Impact of Residual Carbon on Avalanche Voltage and Stability of Polarization-Induced Vertical GaN p-n Junction

Elena Fabris, Carlo De Santi, Alessandro Caria, Kalparupa Mukherjee, Kazuki Nomoto, Zongyang Hu, Wenshen Li, Xiang Gao, Hugues Marchand, Debdeep Jena, Huili Grace Xing, Gaudenzio Meneghesso, Enrico Zanoni, and Matteo Meneghini

***Abstract*— We demonstrate that the residual carbon concentration in the drift region can have a significant impact on the reverse leakage, breakdown voltage, and breakdown stability of GaN-on-GaN vertical diodes. Two generations (Gen1, Gen2) of polarization-doped p-n junctions with different C concentrations were compared, in terms of avalanche voltage, avalanche instability, and deep-level concentration. The original results collected within this paper show that: 1) both generations of devices can safely reach the avalanche regime; diodes with a lower residual $C_N$ have a higher reverse leakage and a lower avalanche voltage, due to an uneven distribution of the electric field; 2) the presence of residual carbon can lead to breakdown walkout, i.e. a recoverable increase in breakdown voltage under reverse-bias stress. Specifically, devices with higher C concentration show a fully-recoverable breakdown walk-out, whereas the breakdown voltage is stable in devices with lower C concentration; and 3) steady-state photocapacitance measurements confirm the presence of $C_N$ in both generations, and are used to assess the relative difference in concentration between Gen1 and Gen2, even for levels below secondary ion mass spectroscopy (SIMS) sensitivity. The results described in this paper indicate the existence of a trade-off between breakdown voltage (increasing by improving compensation) and breakdown stability (improving by reducing $C_N$ concentration) and are of fundamental importance for the optimization of GaN power devices.**

***Index Terms*— Avalanche, breakdown, carbon, gallium nitride, p-n junction, vertical diodes, wide bandgap.**

Manuscript received January 27, 2020; revised March 25, 2020 and April 21, 2020; accepted April 22, 2020. Date of publication June 1, 2020; date of current version September 22, 2020. This research activity was partly funded by project "Novel vertical GaN-devices for next generation power conversion," NoveGaN (University of Padova), through the STARS CoG Grants call. At University of Padova, this work was supported in part by the project INTERNET OF THINGS: SVILUPPI METODOLOGICI, TECNOLOGICI E APPLICATIVI, co-founded (2018–2022) by the Italian Ministry of Education, Universities and Research (MIUR) under the aegis of the "Fondo per il finanziamento dei dipartimenti universitari di eccellenza." The GaN p-n diodes were developed under the ARPAe SWITCHES project at Cornell University, which made use of the Cornell Nanoscale Science and Technology Facilities (CNF) sponsored by the NSF National Nanotechnology Coordinated Infrastructure (NNCI) program (ECCS-1542081), and the Cornell Center for Materials Research Shared Facilities which are supported through the NSF Cornell Center for Materials Research (MRSEC) program (DMR-1719875), as well as NSF Development of an Apertureless Near-Field Scanning Optical and Magneto-Optical Kerr Effect Microscope for Nano-Science Applications (MRI)-1338010. The review of this article was arranged by Editor Y. Cao.
*(Corresponding author: Elena Fabris.)*

Elena Fabris, Carlo De Santi, Alessandro Caria, Kalparupa Mukherjee, Gaudenzio Meneghesso, Enrico Zanoni, and Matteo Meneghini are with the Department of Information Engineering, University of Padova, 35131 Padua, Italy (e-mail: elena.fabris@dei.unip.it; matteo.meneghini@dei.unipd.it).

Kazuki Nomoto, Zongyang Hu, and Wenshen Li are with the School of Electrical and Computer Engineering, Cornell University, Ithaca, NY 14853 USA.

Xiang Gao and Hugues Marchand are with IQE RF LLC, Somerset, NJ 08873 USA.

Debdeep Jena and Huili Grace Xing are with the Department of Materials Science and Engineering, School of Electrical and Computer Engineering, Kavli Institute at Cornell for Nanoscience, Cornell University, Ithaca, NY 14853 USA.

Color versions of one or more of the figures in this article are available online at http://ieeexplore.ieee.org.

Digital Object Identifier 10.1109/TED.2020.2993192

## I. Introduction

VERTICAL GaN devices are promising for next-generation power electronics, thanks to the high current densities and breakdown voltages. The basic units of vertical transistors are the GaN-on-GaN diodes, and diodes with avalanche capability are strongly desired for the development of high-voltage devices. Despite the relevance of the topic, only a few papers investigated the avalanche regime of vertical GaN diodes (see for instance [1]–[7]), and the dependence of avalanche voltage on material and device properties still has to be described in detail. In addition, the stability of devices in the avalanche regime has been investigated only preliminarily [7].

The aim of this work is to contribute to the understanding of the physical processes responsible for avalanche and breakdown walkout in GaN-on-GaN vertical diodes. The focus is on the impact of residual carbon concentration on leakage current, breakdown voltage, and breakdown stability.

## II. Experimental Details

This study was carried out on polarization-doped GaN-on-GaN diodes, which are currently emerging as an alternative to impurity-doped p-n diodes. These devices allow obtaining a higher breakdown voltage, thanks to the larger bandgap of the AlGaN, and no-carrier freeze-out when the temperature decreases, thanks to the contribution of polarization charge to free carrier density [8], [9]. In addition, they are expected to have a faster dynamic response, since p-type conductivity is not obtained through the use of the deep Mg acceptor [10].

0018-9383 © 2020 IEEE. Personal use is permitted, but republication/redistribution requires IEEE permission.
See https://www.ieee.org/publications/rights/index.html for more information.

Authorized licensed use limited to: Cornell University Library. Downloaded on September 24,2020 at 01:54:04 UTC from IEEE Xplore. Restrictions apply.

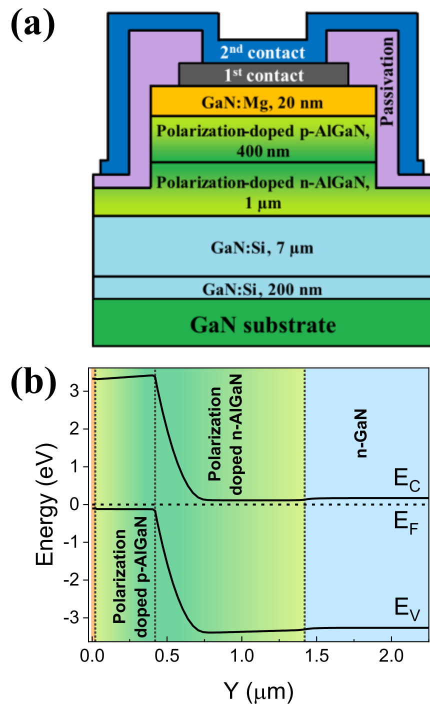


Fig. 1. (a) Structure of the devices under test. (b) Band diagram of a polarization-doped GaN-based p-n diode.

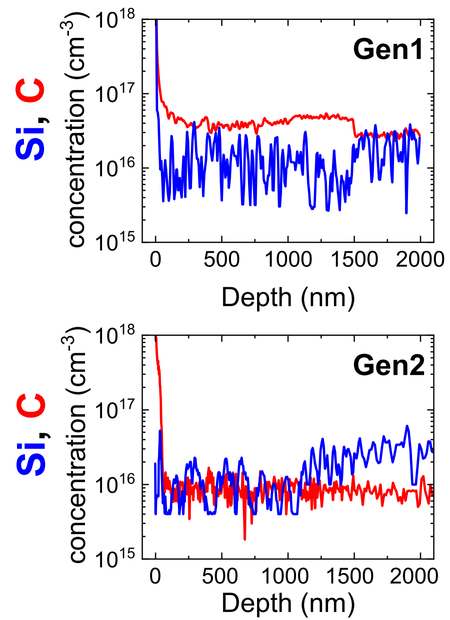


Fig. 2. SIMS data of the devices of Gen1 and Gen2 under test; the blue curve is the silicon concentration and the red curve the carbon concentration.

A schematic representation of the devices under test and the corresponding band diagram are shown in Fig. 1; we studied two generations of polarization-doped p-n diodes grown by metal-organic chemical vapor deposition (MOCVD) with the same structure. On a GaN substrate, five layers consisting of a Si-doped $n^+$ GaN layer (200 nm) with a doping $N_D \sim 10^{18}$ cm$^{-3}$, a Si-doped n-GaN layer (7 $\mu$m) with a doping $N_D \sim 2 \times 10^{16}$ cm$^{-3}$, a n-type linearly graded AlGaN layer with the Al composition graded up from 0% to 5.6% (1 $\mu$m), a p-type linearly graded AlGaN layer with the opposite Al composition gradient (from 5.6% to 0%) (0.4 $\mu$m), and Mg-doped p GaN layer (20 nm) with a doping higher than $10^{20}$ cm$^{-3}$ were grown. The analyzed diodes were optimized for high breakdown voltage through the use of a field plate [4], [11]. In the devices under test, no intentional carbon doping is present, but a residual concentration was detected by secondary ion mass spectroscopy (SIMS) (Fig. 2). The difference between the two generations lies in the fact that Gen1 samples have a much higher carbon concentration in the drift layer, compared to Gen2 devices.

## III. Experimental Results

Since for Gen2 devices the carbon concentration is below the SIMS sensitivity limit, we carried out steady-state photocapacitance measurements (SSPC) to evaluate the presence and density of carbon in the drift region, and the difference in concentration in Gen1 and Gen2 devices. The measurement consists of the analysis of the capacitance transients induced by exposure to monochromatic light of increasing photon energy between 1.5 and 3.6 eV. The results of SSPC measurements are reported in Fig. 3. By analyzing the steady-state photocapacitance spectrum reported in Fig. 4,

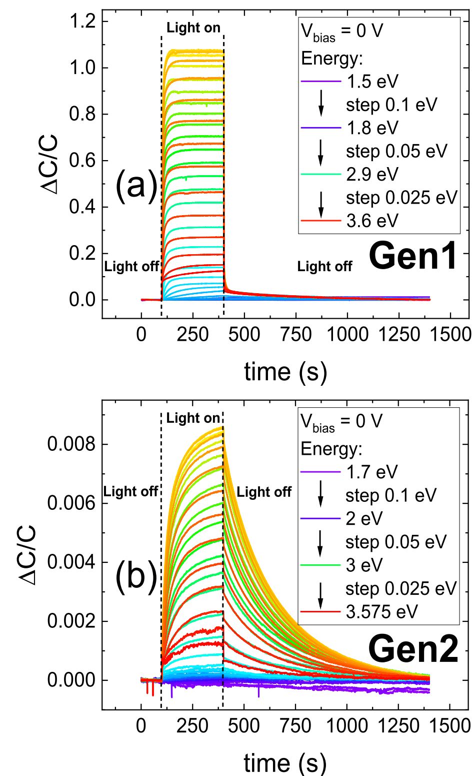


Fig. 3. Capacitance transients obtained using different wavelengths of monochromatic incident light during SSPC measurements in the devices of (a) first generation and (b) second generation.

a change in the slope of the SSPC spectrum is visible at about 2.5 eV both in Gen1 and Gen2 devices, indicating an emission process of carriers from a deep level located 2.5 eV below the conduction band. This is consistent with the level attributed to substitutional carbon ($C_N$) defects [12]. The results of these measurements show that Gen2 devices have a

Authorized licensed use limited to: Cornell University Library. Downloaded on September 24,2020 at 01:54:04 UTC from IEEE Xplore. Restrictions apply.

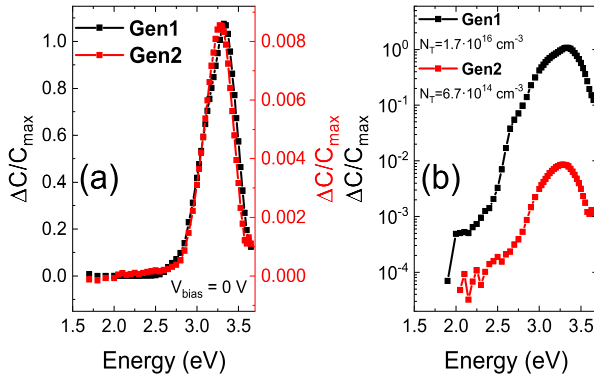


Fig. 4. Comparison between the steady-state photocapacitance spectrum in (a) linear scale and (b) semilog scale in the two sets of devices; a change in the slope of the steady-state photocapacitance spectrum is visible at ∼2.5 eV both in Gen1 and Gen2.

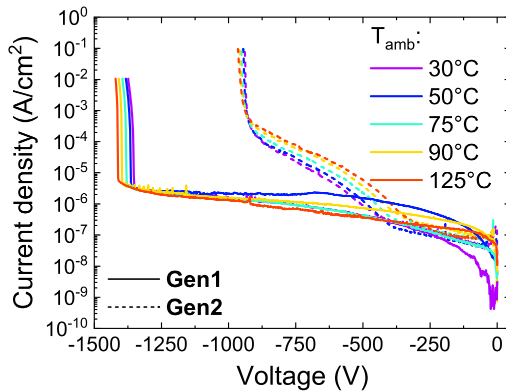


Fig. 5. *I–V* characteristics at different temperatures of devices of the first generation (solid lines) and second generation (dotted lines).

much lower $C_N$ density; for Gen1 and Gen2, concentrations of $1.7 \times 10^{16}$ cm$^{-3}$ and $6.7 \times 10^{14}$ cm$^{-3}$ were extracted (Fig. 4). Therefore, SSPC has been proved to be an effective method for evaluating carbon density at low concentrations, close to the sensitivity of SIMS; the values obtained by SSPC represent the $C_N$ concentration, differently from SIMS, which gives the chemical concentration. Results demonstrate that Gen2 devices have a much lower residual carbon compared to Gen1.

The avalanche capability of the polarization-doped diodes was investigated by means of *I–V* characterization under reverse bias at different temperatures. The two generations of diodes show a different behavior, as can be seen in Fig. 5.

Gen1 devices have a low leakage current up to a breakdown voltage about equal −1370 V (30 °C); by analyzing the reverse voltage for a current density of −100 mA/cm$^2$, a positive temperature coefficient is found, with a slope of 0.50 V/°C [see Fig. 6(a)], suggesting the presence of impact ionization [6], [7]. On the other hand, Gen2 devices show a higher leakage current and a lower avalanche voltage (−935 V at 30 °C). The temperature coefficient is still positive, but with a slope of 0.27 V/°C [see Fig. 6(b)] (calculated for a current density of −100 mA/cm$^2$), slightly lower than Gen1 and previous articles dealing with avalanche capable GaN-on-GaN p-n diodes [1], [3]. Therefore, the first generation of samples

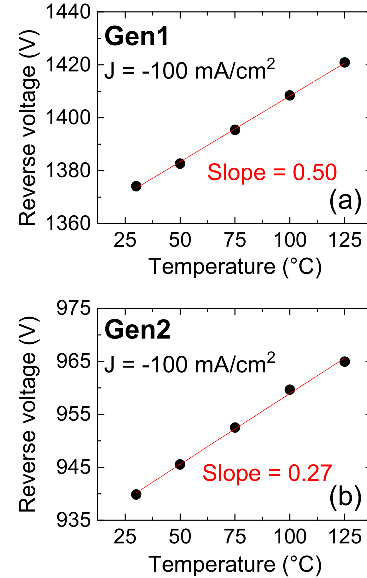


Fig. 6. Dependence of breakdown voltage on temperature; the temperature coefficient is positive with a slope of (a) 0.50 V/°C for the devices of the first generation and (b) 0.27 V/°C for the devices of the second generation.

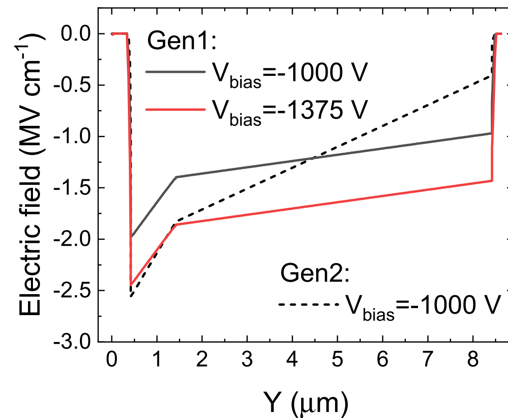


Fig. 7. Electric field distribution in the devices of Gen1 (solid lines) and Gen2 (dotted line) calculated by using numerical TCAD simulations.

has a higher breakdown voltage and lower leakage. To deeply understand the difference in breakdown voltage and leakage current in the two generations, numerical technology computer-aided design (TCAD) simulations were carried out. Fig. 7 reports the electric field at −1000 V for the two devices; as can be noticed, in Gen1 samples, the higher $C_N$ concentration leads to a better compensation of the Si-doped drift region and to a nearly flat electric field profile. On the other hand, the lower $C_N$ density in Gen2 results in a nonideal compensation; the drift region has a n-type conductivity, and the *E*-field shows a marked decreasing trend in the drift region. As a consequence, for the same voltage, Gen2 devices have a much higher electric field than Gen1. At the failure voltage (∼1000 V), the peak field in Gen2 devices is around 2.5 MV/cm. In Gen1, the same field is reached at 1375 V (see Fig. 7), which is close to the experimental failure voltage (Fig. 5).

Another fundamental issue for high reverse voltage operation is the stability of the breakdown voltage during prolonged operation in the avalanche regime. To analyze if the

Authorized licensed use limited to: Cornell University Library. Downloaded on September 24,2020 at 01:54:04 UTC from IEEE Xplore. Restrictions apply.

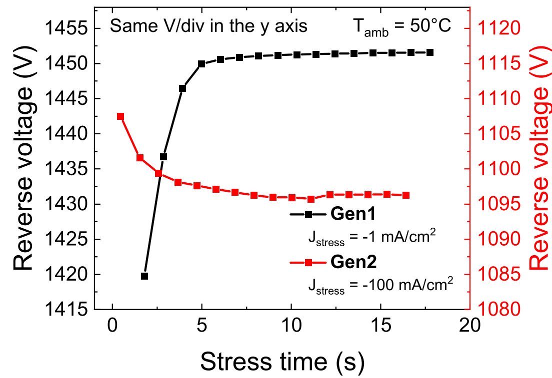


Fig. 8. Time-dependence of breakdown voltage at 50 °C. The breakdown voltage increases during the stress time ($J_{stress}$ = −1 mA/cm$^2$) in the first generation (black curve) and decreases during the stress time ($J_{stress}$−100 mA/cm$^2$) in the second generation (red curve).

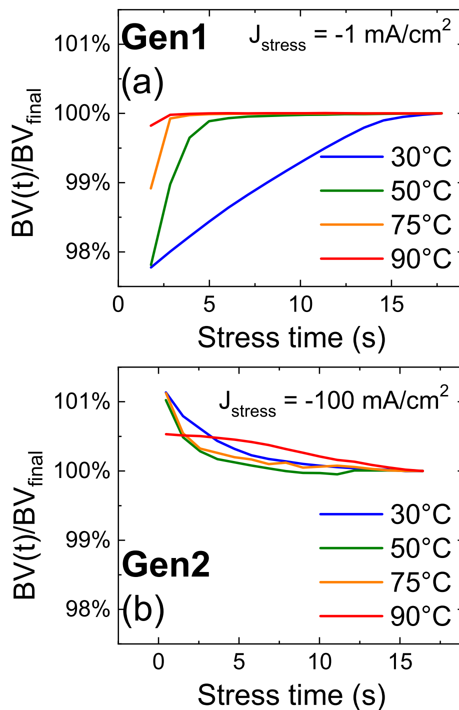


Fig. 9. Ratio between the breakdown voltage during stress [BV(t)] and the breakdown voltage at the end of the stress ($BV_{final}$) as a function of time (a) in the first generation and (b) in the second generation at different temperatures.

breakdown voltage was stable, the devices were submitted to a constant current stress for a relatively long time in avalanche conditions (with a current density $J_{stress} = -1$ mA/cm$^2$ and $-100$ mA/cm$^2$ for Gen1 and Gen2, respectively, i.e. a current level two order of magnitude higher than the current corresponding to the onset of the avalanche mechanism) and the measurements were repeated at different ambient temperatures. The devices of the two generations exhibit a substantially different behavior of the time-dependence of the breakdown voltage under the avalanche regime (Figs. 8 and 9). In particular, for Gen1 devices, the stress in the avalanche regime causes an increase in the breakdown voltage with increasing stress time [Figs. 8 and 9(a)]. This effect is known as breakdown walkout [13]–[15] and, according to [6] and [7], could originate from the time-dependent ionization of carbon acceptors, induced by the high reverse bias. Once more and more $C_N$ atoms are ionized, the increased Coulomb and phonon scattering reduces the mean-free path, thus leading to an increase in breakdown voltage. In [6] and [7], no experimental demonstration of the role of carbon on the avalanche walkout was given.

The results in Figs. 8 and 9 clearly confirm that the density of carbon impacts on the stability of avalanche voltage. Remarkably, Gen2 devices showed a small decrease in the breakdown voltage during operation in the avalanche regime [Figs. 8 and 9(b)]. Similar behavior was observed also by Rackauskas *et al.* [16] and was ascribed to impurity band conduction along dislocations. The absolute variation in breakdown voltage is much lower in Gen2 devices, thus indicating better stability in avalanche regime.

## IV. Conclusion

In summary, we demonstrated the existence of a trade-off between leakage current, breakdown voltage, and breakdown stability, depending on the residual carbon concentration in polarization-doped (Al)GaN vertical p-n diodes. Lowering the residual carbon improves the stability of breakdown voltage, but leads to an increase in the leakage and a decrease in breakdown limit. This is because lowering $C_N$ concentration results in a non-optimized compensation of the drift region, with consequences on the electric field distribution. The $C_N$ concentrations in the two sets of samples were analyzed by means of SSPC measurements, which has been proved to effectively estimate $C_N$ density below the SIMS sensitivity limit.

## References


[1] I. C. Kizilyalli, A. P. Edwards, H. Nie, D. Disney, and D. Bour, "High voltage vertical GaN p-n diodes with avalanche capability," *IEEE Trans. Electron Devices*, vol. 60, no. 10, pp. 3067–3070, Oct. 2013, doi: 10.1109/TED.2013.2266664.

[2] O. Aktas and I. C. Kizilyalli, "Avalanche capability of vertical GaN p-n junctions on bulk GaN substrates," *IEEE Electron Device Lett.*, vol. 36, no. 9, pp. 890–892, Sep. 2015, doi: 10.1109/LED.2015.2456914.

[3] Z. Hu *et al.*, "Near unity ideality factor and Shockley-Read-Hall lifetime in GaN-on-GaN p-n diodes with avalanche breakdown," *Appl. Phys. Lett.*, vol. 107, no. 24, Dec. 2015, Art. no. 243501, doi: 10.1063/1.4937436.

[4] K. Nomoto *et al.*, "1.7-kV and 0.55-mΩ·cm$^2$ GaN p-n diodes on bulk GaN substrates with avalanche capability," *IEEE Electron Device Lett.*, vol. 37, no. 2, pp. 161–164, Feb. 2016, doi: 10.1109/LED.2015.2506638.

[5] L. Cao *et al.*, "Experimental characterization of impact ionization coefficients for electrons and holes in GaN grown on bulk GaN substrates," *Appl. Phys. Lett.*, vol. 112, no. 26, Jun. 2018, Art. no. 262103, doi: 10.1063/1.5031785.

[6] C. De Santi *et al.*, "Demonstration of avalanche capability in polarization-doped vertical GaN pn diodes: Study of walkout due to residual carbon concentration," in *IEDM Tech. Dig.*, Dec. 2018, pp. 30.2.1–30.2.4, doi: 10.1109/IEDM.2018.8614568.

[7] E. Fabris *et al.*, "Breakdown walkout in polarization-doped vertical GaN diodes," *IEEE Trans. Electron Devices*, vol. 66, no. 11, pp. 4597–4603, Nov. 2019, doi: 10.1109/TED.2019.2943014.

[8] H. G. Xing *et al.*, "Unique opportunity to harness polarization in GaN to override the conventional power electronics figure-of-merits," in *Proc. 73rd Annu. Device Res. Conf. (DRC)*, Jun. 2015, pp. 51–52, doi: 10.1109/DRC.2015.7175549.


Authorized licensed use limited to: Cornell University Library. Downloaded on September 24,2020 at 01:54:04 UTC from IEEE Xplore. Restrictions apply.

[9] J. Simon, V. Protasenko, C. Lian, H. Xing, and D. Jena, "Polarization-induced hole doping in wide-band-gap uniaxial semiconductor heterostructures," *Science*, vol. 327, no. 5961, pp. 60–64, Jan. 2010, doi: 10.1126/science.1183226.

[10] P. Kozodoy, S. P. DenBaars, and U. K. Mishra, "Depletion region effects in Mg-doped GaN," *J. Appl. Phys.*, vol. 87, no. 2, pp. 770–775, Jan. 2000, doi: 10.1063/1.371939.

[11] K. Nomoto *et al.*, "GaN-on-GaN p-n power diodes with 3.48 kV and 0.95 $\Omega$-cm$^2$: A record high figure-of-merit of 12.8 GW/cm$^2$," in *IEDM Tech. Dig.*, Dec. 2015, doi: 10.1109/IEDM.2015.7409665.

[12] J. L. Lyons, A. Janotti, and C. G. Van de Walle, "Effects of carbon on the electrical and optical properties of InN, GaN, and AlN," *Phys. Rev. B, Condens. Matter*, vol. 89, no. 3, Jan. 2014, Art. no. 035204, doi: 10.1103/PhysRevB.89.035204.

[13] W. L. Guo, R.-S. Huang, L. Z. Zheng, and Y. C. Song, "Walkout in p-n junctions including charge trapping saturation," *IEEE Trans. Electron Devices*, vol. 34, no. 8, pp. 1788–1794, Aug. 1987, doi: 10.1109/T-ED.1987.23152.

[14] P. C. Chao, M. Shur, M. Y. Kao, and B. R. Lee, "Breakdown walkout in AlAs/GaAs HEMTs," *IEEE Trans. Electron Devices*, vol. 39, no. 3, pp. 738–740, Mar. 1992, doi: 10.1109/16.123504.

[15] W.-B. Tang and Y.-M. Hsin, "Reversible off-state breakdown walkout in passivated AlGaAs/InGaAs PHEMTs," *IEEE Trans. Device Mater. Rel.*, vol. 6, no. 1, pp. 42–45, Mar. 2006, doi: 10.1109/TDMR.2006.870345.

[16] B. Rackauskas, S. Dalcanale, M. J. Uren, T. Kachi, and M. Kuball, "Leakage mechanisms in GaN-on-GaN vertical pn diodes," *Appl. Phys. Lett.*, vol. 112, no. 23, Jun. 2018, Art. no. 233501, doi: 10.1063/1.5033436.

Authorized licensed use limited to: Cornell University Library. Downloaded on September 24,2020 at 01:54:04 UTC from IEEE Xplore. Restrictions apply.